Tunable Wetting of Titanium and Gold Based Wicking Materials -For Uses under High Accelerations

C. Ding*, P. Bozorgi**, C.D. Meinhart**, and N.C. MacDonald**

*California Nanosystems Institute, UCSB
Room 2229, ESB, Santa Barbara, CA 93106, USA, ding@engr.ucsb.edu
**Mechanical Engineering Dept., University of California, Santa Barbara, CA, USA

ABSTRACT

Heat pipes adopt wicking materials to achieve some unique functions that thermal siphons could not achieve [1]. Based on titanium micromachining, gold plating and surface modification techniques, we fabricated pillar arrays, and modify the dimension or parameters to investigate their tunable wicking behaviors. Our study shows that water completely wets the micro/nano-scale titania structures fabricated with micromachining and surface modification techniques, and the spreading trends of water were found to be diffusive. Wicking material under different acceleration conditions were also investigated and we found the bitextured titania structures (BTS) undergoes twice larger inertia force than the monostructures with same dimensions.

Keywords: Bitextured nanostructure titania, wetting, acceleration, cooling, titanium.

1 INTRODUCTION

Wicking materials are widely used in heat pipes which have long been utilized for cooling microprocessor chips [2, 3], nuclear power systems, space based radar systems, etc.. Heat pipes have been of particular useful in cooling highly power intensive chips because of their high thermal conductivity and the capacity to carry high amounts of heat. The working fluid evaporates after absorbing heat from the hot end and flows towards the cold end, condensing thereby. A very fine wick structure on the internal wall of the heat pipe brings the condensate back from the cold end towards the hot end by capillary actions.

A flat heat pipe has wicking materials on the interior walls of its chamber to automatically pump the cooling fluids from the heat sink side to the evaporator side when transporting heat. The flat geometry allows micro/nano-scale machining techniques to be applied for forming unique wicking materials such as nanowires, carbon nanotubes, biporous copper, micromachined structures, etc. The wicking material is usually designed to provide high capillary force on the spreading liquid. The capillary force can be derived using virtual energy method when a working fluid contacts with a solid surface. Although capillary can be well defined, the friction force between fluid and solid surfaces is relatively difficult to measure and analytically to define for complicated structures. For some application such as the wicking material in spacecraft based cooling systems may undergo a certain range of accelerations which may induce another term of force due to inertia. Wetting behaviors of wicks can be dramatically changed because of inertia forces depending how the device is aligned according to acceleration direction.

1.1 Wetting and Roughness

When a droplet of fluid such as water contacts with a smooth and flat surface (Fig. 1A), hydrophobicity or hydrophilicity is governed by the relative reaction of the forces at the triple line arising from the three interfacial energies (or call surface tensions), γ_{SV}, γ_{SL}, and γ, taking place at the solid-vapor, solid-liquid, and liquid-vapor interfaces, respectively. Projecting these three surface tensions acting on a specific contact line gives the Young's equation:

$$\cos\theta_e = \frac{\gamma_{SV} - \gamma_{SL}}{\gamma} \quad (1)$$

where θ_e is the equilibrium contact angle.

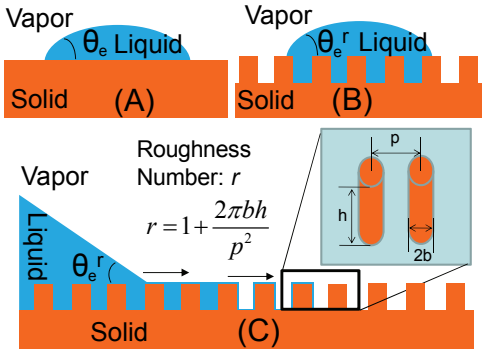

Figure 1: Flow of the impregnating film at the front boundary. Figure A shows the Young's contact angle; Figure B and C show the static and dynamic cases of the wetting on solid surfaces.

In reality it usually differs from this ideal situation in which we have smooth and clean surface. Solid surfaces are usually rough or carry undulations, pores, surface defects. Using virtual energy method together with Young's equation we can derived to get the Wenzel's relation [4]:

$$\cos\theta_e^r = r\cos\theta_e \quad (2)$$

where θ_e^r is the apparent contact angle. The above equation comes with a limit of $-1 \le r\cos\theta_e \le 1$. The Wenzel's relation tells us that the surface roughness can enhance both the nonwetting (hydrophobic) and wetting (hydrophilic) ability of liquid on solid surfaces. When the Young's contact angle on flat/smooth surface is less than $90°$, roughness will reduce the apparent contact angle leading to superhydrophilic/superwetting case [5-7].

1.2 Statics and dynamics

In the previous subsection we show that the roughness modifies the value of apparent contact angle, and super-wetting can be possibly achieved by tuning the roughness. A simple idea is to use micromachined pillars to obtain large surface roughness and optimize the wetting by tuning the pillar dimensions. We denote such a surface by its pillar roughness r which is defined in Fig. 1. Provided that the case in Fig. 1, the pillars guide the liquid within the pillar arrays and form in a manner similar to wicking but more accurately hemiwicking which is intermediate between spreading and imbibition [8]. Assuming that the top surface areas can also get wet during the progression of the liquid film the surface energy change is then only due to the suppression of the liquid-vapor interfaces. Using virtual energy method again, the capillary force is given by [9, 10]:

$$F_{cp} = \gamma(r-1) = \frac{2\pi\gamma bh}{p^2} \quad (3)$$

The capillary force is then constant and depends only on the surface roughness. This force is generally resisted by viscous force due to the flow of liquid. When the wicking material works under accelerations, then the inertial force will get involved when the liquid wets or de-wets. The net driving force for wetting of fluids on wicks will be a sum of the following three forces:

$$F_{net} = F_{cp} - F_{friction} \pm F_{inertia} \quad (4)$$

where the inertial force may help increase of decrease the net force depending on how the wetting direction is aligned with the acceleration direction. The resistance force to the flow generally comes from two domains: 1) velocity gradients over a distance h due to the friction between the bottom surface and the moving fluid; 2) the perturbation to the flow by the pillars arrays. These two resistant force shall be both present during the flow, but one may dominate the other for different designs (for example, the pillar height difference) of the micro patterns. No accurate general rule is available at this point to predict the flow behavior because of the wide variety of surface properties. However, balancing the driving force with the viscous force, the dynamic behavior of the flow on rough solids was found to obey the famous Washburn relation [11] which stipulates the travel path of the flow increases as the square root of time: $x=(Dt)^{1/2}$ where D is the dynamic coefficient of the flow. A high dynamical coefficient is preferred for the wicking material (pillar arrays) used in heat pipes for ensuring acceptable operations. It'll be interesting to find out the dynamic coefficient experimentally, and provide insightful information for optimizing it by tuning the design parameters.

2 FBARICATION

2.1 Dry Etching and Surface Oxidization

Based on titanium micromachining and surface modification techniques, we fabricated BTS with two main designs: 5μm/5μm (Dia./Gap) and 100μm/50μm (Dia./Gap) with an etch depth of 50μm. The fabrication process for making BTS (Fig. 2 and Fig. 3C) begins with the SiO_2-masked deep etching of a 300 μm thick Ti substrate using Inductively Coupled Plasma (ICP) etch in an Ar/Cl_2 ambience. The SiO_2 layer is approximately 3 μm thick. After deep etching is complete, the sample is oxidized in a 30% solution of hydrogen peroxide at ~83^0C for 15-20minutes to obtain the BTS and the bottom floor surface. The surfaces show nano-scale walls (30~50nm thick) and pores (150~200nm in diameter). The nanostructures are self assembled on high-aspect-ratio Ti pillar arrays when oxidized in H_2O_2 solution.

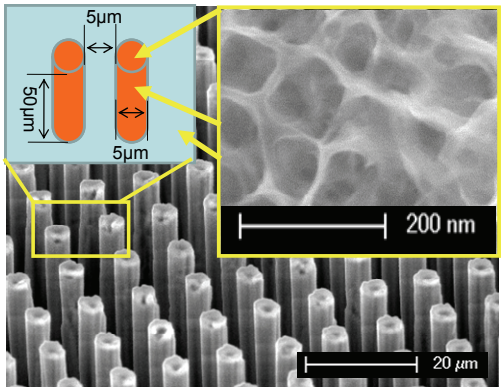

Figure 2: SEM photograph of the BTS with 5μm/5μm (Dia./Gap). The height of the pillars is ~50μm.

2.2 Gold Plating

The sample (Fig. 3C) is further processed for gold plating. After forming BTS on the Ti pillars, a seed layer (20nm Ti/150nm Au) was deposited on all surfaces then it was dipped into a non-cyanide based solution for Au plating at 55^0C. A current 3mA/cm^2 was applied during plating. The sample was taken out for SEM study after plating for 7600 seconds (Fig. 3D). The minimum gap was reduced from 50μm to 5μm after 7600 seconds plating.

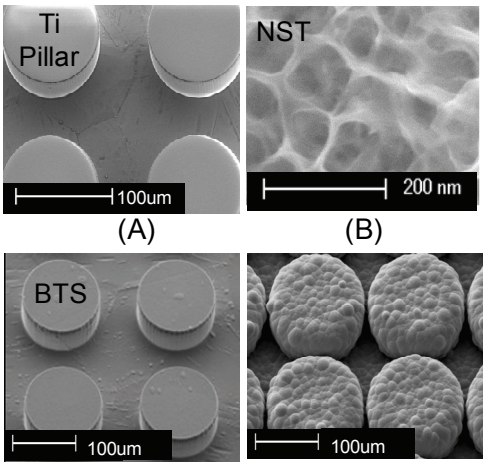

Figure 3: SEM photographs of Ti pillars (A), nanostructure titania-NST (B), bitextured titania structure-BTS (C), and BTS with plated gold (D).

3 EXPERIMENTS AND RESULTS

3.1 Wetting Experiments and Analysis

DI water was used as a working fluid for its high merit number [12] for heat pipe systems. The experiment was done by bringing the wicks into contact with a drop of water (~40μL), and the flow is recorded with a camera (Nikon D90). The position of the front liquid interface was extracted by decomposing the video into 24 frames/second. The drop completely wetted the nano/micro structured surface at the end, and the contact angle goes to zero. A curve of the form $x^2 = Dt$ is well fitted to the collected distance-vs-time data shown in Fig. 4. The experimental data generate the dynamic coefficients, D, for different wetting experiments. By differentiating the fitted curve we get the wetting speed:

$$\frac{dx}{dt} = \frac{D}{2}\frac{1}{x} \qquad (5)$$

The velocity plot of each experiment is shown in Fig. 5.

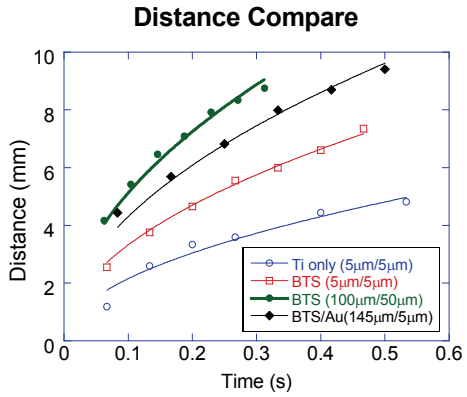

Figure 4: This plot shows the capillary flow front interface path as a function of time.

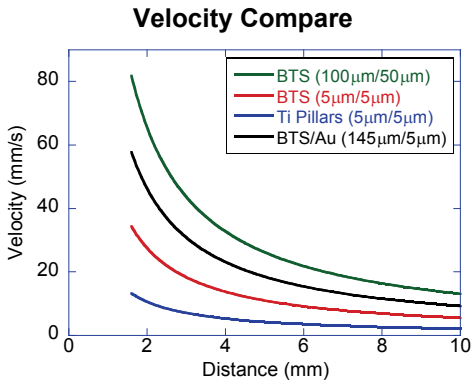

Figure 5: Velocity plot of equation (5) for four wicks.

As shown in Fig. 5, the NST enhanced the wetting due to the increased surface roughness for the same design parameter (5μm Dia./5μm gap). However a different design parameter (100μm Dia./50μm gap) gives over ~160% improvement. Further tuning of the design parameter by gold plating reduced the velocity by a small amount.

3.2 Acceleration Tests and Discussions

The wetting performances of the wicking material under acceleration conditions are tested with Ideal Aerosmith acceleration table (Model: 1291BR). A schematic of the testing setup with this testing system is shown in Fig. 6. The sample is fixed at one end of the extension arm to be 0.25m away from the axis of the rotation. A drop of 30μL of DI water is used to completely wet the wicks from the distal end to the near-to-rotation-center end of the wicking substrate. A transparent cover (3.5cm in diameter, 1cm in height) was fixed on top of the sample to reduce evaporation when the device is under acceleration and jogging. The angular acceleration rate is set to be 300 $^o/s^2$, and this rate is used in each test for comparison. We chose the sample as shown in Fig. 3A and 3C for experiments for their relatively lower capillary pressure due to their larger dimension both in diameter and gap.

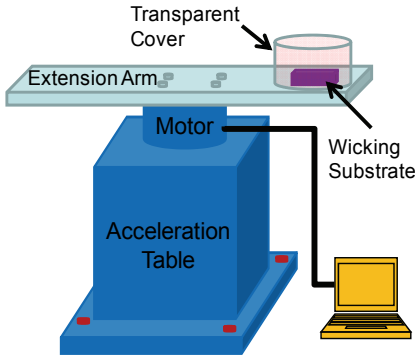

Figure 6: Schematic of the acceleration testing systems.

The goal of the experiments is to see if they can keep the wick wet under 10g jogging acceleration at radial

direction when wetting from the distal end of the extension arm to the center. The sample was accelerated at an increasing and decreasing angular acceleration rate both at $300^{o}/s^{2}$ to get a specific jogging acceleration in radial direction, and then kept at certain jogging speed for 10 seconds.

The wicking substrate with pure Ti pillars was found to be able to undergo a radial acceleration of ~6.3g where g stands for gravity acceleration, above this rate dry area was found as shown in Fig. 7A. The sample as shown in Fig. 3C with BTS was found to be able to undergo up to a radial acceleration of 12.13g. Part of the water volume is found gone during spin due to evaporation or flying so that the total volume of water is reduced. A well-sealed device would help avoid reduction of water volume.

From the analysis of in section 1.2 we know that when a drop of water is put contact with BTS wicks the spreading volume of water undergoes both capillary force and viscous force. When the device is under zero acceleration the capillary force helps increase the wetting speed while the viscous force functions as to decrease the speed. Experimental wetting results in Fig. 5 show that a design in favor of increasing speed is possible by forming BTS or changing the dimensions of the micromachined wicking structures. When the wicking substrate is under acceleration as in Fig. 6 both the capillary force and viscous force help to be in favor of fighting with de-wetting flows. With this specific situation shown in Fig. 6 BTS not only helps increase capillary force but may also helps increase viscous force for avoiding de-wetting.

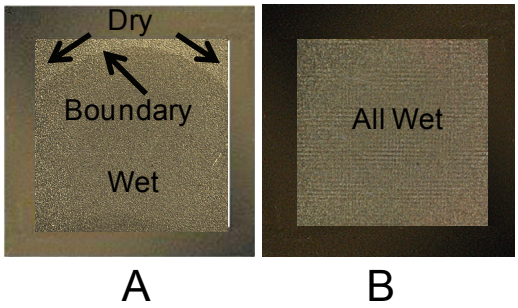

Figure 7: Acceleration (10g) test result comparison between Ti mono-structure (A) and BTS (B). Figure A shows the dry-out around the two top corners. Figure B shows that all areas stay wet due to BTS.

4 CONCLUSIONS

Complete wetting of DI water on micromachined titanium structures is achieved, and the spreading trends of water were found to be diffusive. Wetting on titanium based microstructures was improved by oxidizing the titanium pillars and forming bitextured titania structures. The nanoscale titania structure greatly enhances the wetting dynamics by ~160%. A dimension change from 5μm/5μm (Dia./gap) to 100μm/100μm provides much higher wetting speed. This indicates that the wetting velocity of wicking material can be tuned dramatically by adopting nanostructures and dimension changes. Two wicking material were investigated under different acceleration conditions for studying of de-wetting behaviors, and we found all the bitextured titania structures (BTS) can keep wet under much larger radial acceleration (12.13g) than the monostructures (6.3g) with same dimensions.

This work is supported by the TGP program under the Microsystems Technology Office at the Defense Advanced Research Projects Agency. A portion of this work was done in the UCSB nanofabrication facility, part of the NSF funded NNIN network. The authors would like to thank Timothy J. Reed and Chris Burgner for their help on testing the wicks under accelerations.

REFERENCES

[1] P. D. Dunn and D. A. Reay, "Heat pipe," Physics in Technology, vol. 4, pp. 187-201, 1973.
[2] U. Vadakkan, G. M. Chrysler, and S. Sane, "Silicon/water vapor chamber as heat spreaders for microelectronic packages," IEEE, 2005, pp. 182-186.
[3] H. Xie, H. Xie, A. Ali, and R. Bhatia, "The use of heat pipes in personal computers," ITHERM, 1998
[4] R. N. Wenzel, "Resistance of Solid Surfaces to Wetting by Water," Industrial & Engineering Chemistry, vol. 28, pp. 988-994, 1936.
[5] X. Feng and L. Jiang, "Design and creation of superwetting/antiwetting surfaces," Adv. Mater, vol. 18, pp. 3063-78, 2006.
[6] C. Extrand, S. Moon, P. Hall, and D. Schmidt, "Superwetting of Structured Surfaces," Langmuir, vol. 23, pp. 8882-8890, 2007.
[7] J. Yuan, X. Liu, O. Akbulut, J. Hu, S. Suib, J. Kong, and F. Stellacci, "Superwetting nanowire membranes for selective absorption," Nature Nanotechnology, vol. 3, p. 332, 2008.
[8] D. Quéré,, "Wetting and Roughness," Annual Review of Materials Research, vol. 38, pp. 71-99, 2008.
[9] C. Ishino, M. Reyssat, E. Reyssat, K. Okumura, and D. Quere, "Wicking within forests of micropillars," EPL, vol. 79, p. 56005, 2007.
[10] C. Ding, P. Bozorgi, N. Srivastava, M. Sigurdson, C. D. Meinhart, and N. C. MacDonald, "Super Wetting of Micro&Nano Structured Titania Surfaces," in Transducers, Denver, CO, 2009.
[11] E. W. Washburn, "The Dynamics of Capillary Flow," Physical Review, vol. 17, p. 273, 1921.
[12] W. G. Anderson, J. H. Rosenfeld, D. Angirasa, and Y. Me, "Evaluation of Heat Pipe Working Fluids in the Temperature Range 450 to 700 K," STAIF-04

CONTACT
*C. Ding, Public, tel: +1-805-893-5341;
changsong_ding@yahoo.com